Contents lists available at ScienceDirect

Colloids and Surfaces A: Physicochemical and Engineering Aspects

Layer-by-layer deposition of a TiO₂-filled intumescent coating and its effect on the flame retardancy of polyamide and polyester fabrics

Kadir Apaydin [a,d], Abdelghani Laachachi [a,*], Vincent Ball [b,c], Maude Jimenez [d], Serge Bourbigot [d], David Ruch [a]

[a] Department for Advanced Materials and Structures, Centre de Recherche Public Henri Tudor, 66 rue de Luxembourg, L-4002 Esch-sur-Alzette, Luxembourg
[b] Université de Strasbourg Faculté de Chirurgie Dentaire, 67000 Strasbourg, France
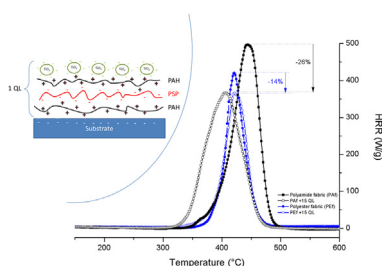[c] Institut National de la Santé et de la Recherche Médicale, Unité Mixte de Recherche 1121, 11 rue Humann, 67085 Strasbourg Cedex, France
[d] UMET-ISP, UMR 8207, ENSCL, UMET UMR CNRS 8207, CS 90108, 59652 Villeneuve d'Ascq Cedex, France

HIGHLIGHTS

- We designed by LbL a new flame retardant coating for plastic fabrics.
- Our coating contains all ingredients of traditional intumescent system.
- The fact that thick coatings 500 nm can be obtained in 1 h only of LbL processing.
- We have found that the efficiency of the coating depends on the kind of fabrics.

GRAPHICAL ABSTRACT

ARTICLE INFO

ABSTRACT

New intumescent flame retardant coating made from poly(allylamine) (PAH), sodium polyphosphates (PSP) and TiO₂ nanoparticles was designed using layer-by-layer assembly. The (PAH-PSP-PAH-TiO₂)$_n$ (where "n" denotes the number of quadralayers) assembly has been deposited on silicon wafers in order to evaluate its thickness as well as its topography by ellipsometry and by atomic force microscopy (AFM), respectively. According to AFM measurements, the coating appears smooth and continuous. The film exhibits a linear growth regime with a thickness of approximately 500 nm for 15 quadralayers (QL). However, when deposited on polyamide or polyester fabrics, this coating displays different morphologies as it was shown by scanning electron microscopy (SEM) analysis. The thermo-oxidative degradation and flammability properties of the coatings and their effect on polyamide and polyester fabrics have been evaluated by thermogravimetric analyses (TGA) and pyrolysis combustion flow calorimeter (PCFC) respectively. We have found that the coating acts efficiently in reducing the peak of the heat release rate (pHRR) value for polyamide fabric while very limited effect was observed on polyester fabric.

© 2014 Elsevier B.V. All rights reserved.

1. Introduction

In recent years, the elaboration of intumescent flame retardant coatings using the layer-by-layer technology (LbL) has become a popular strategy to enhance the reaction to fire of materials such as cotton [1–7], polyester and their blends [2,3,8,9], polylactic acid films [10], polyurethane foams [11], ramie [12] and polyamide 6.6 fabrics [13]. Upon heating the intumescent flame retardant
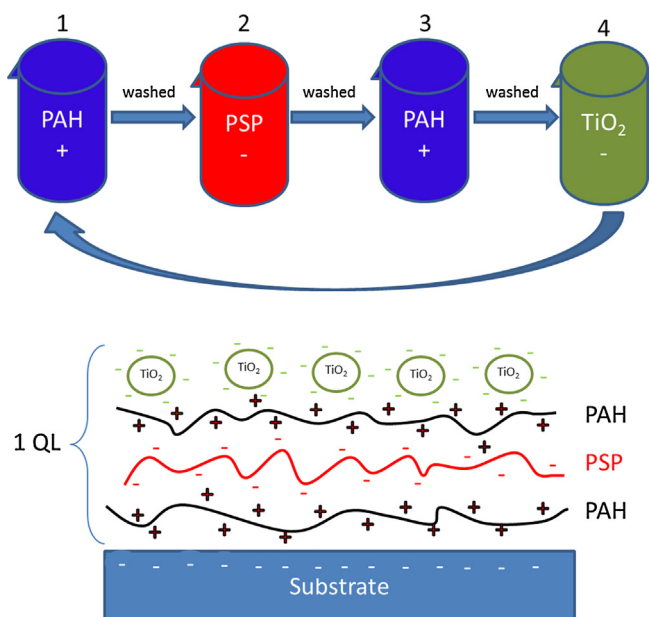
Fig. 1. Schematic representation of layer-by-layer deposition. We repeated the steps 1-4 until the desired number of bilayers.

material swells and forms a carbonaceous char layer at the surface of the material, which acts as a physical barrier limiting the heat, fuel and oxygen transfers between the flame and material. In general, an intumescent system is constituted of three main ingredients [14]: (i) a carbon source mainly polymer-substrate, (ii) an acid source such as polyphosphate (PSP), (iii) a swelling agent such as melamine, poly(allylamine), isocyanurate.... Beyond these ingredients, inorganic fillers such as clays, metal oxides can also be used to reinforce the formed char layer. Intumescent system can be applied on wide range of substrates implying the use of different processing techniques. Hence, due to its effectiveness, numerous scientists have chosen to combine layer-by-layer technique with the intumescent concept to design new thin flame retardant coatings in order to improve the reaction of textiles to fire. For example, in order to improve the reaction of cotton fabric to fire, Grunlan's group [1,4,7] designed three different intumescent coatings: (poly(allylamine)/poly(sodium phosphate)) [1], (chitosan/phytic acid) [4] and (branched polyethylenimine/urea/diammonium phosphate) [7]. Furthermore, Huang et al. [5] developed a (polyacrylamide/exfoliated graphene oxide) LbL system stabilized by hydrogen-bonding interactions which is able to decrease the peak heat release rate (pHRR) by 50% and to increase the time to ignition by 56% (according to the cone calorimeter results) [5]. Similarly, Malucelli and coworkers [6] studied the effect of deoxyribonucleic acid (DNA) coupled with chitosan to improve the fire performance of cotton fabric. This green LbL system, which was self-extinguishing during horizontal flammability tests, permits to reduce the pHRR by 40%, while increasing the limiting oxygen index (LOI) up to 24% [6]. In other efforts, Malucelli's group [2,3,8,9] has also shown that it is possible to enhance the fire retardant properties of cotton, polyester and their blends using ammonium polyphosphate (APP) based coatings. Moreover Zhang et al. [12] have constructed intumescent coating based on APP with amino-functionalized multiwall carbon nanotubes to enhance the reaction to fire of ramie fabric [12]. Using the layer-by-layer technique, Laachachi et al. [10] and Cain et al. [11] elaborated intumescent coating including poly(allylamine)/montmorillonite/polyphosphate compounds to protect polylactic acid films and polyurethane foams, respectively. Recently we have studied the effect of

poly(allylamine)/polyphosphate coatings on polyamide fabrics [13] and demonstrated the effectiveness of these coating in enhancing the thermal stability and improved the reaction to fire (pHRR decrease up to 36%) [13].

Polyamide 6.6 and polyester fabrics are two thermoplastic materials used in many fields such as clothing, transport, building, etc. These materials are highly flammable whereas legislation very often requires low flammability. In order to overcome this drawback and improve their inflammability, we used in the present work a ternary intumescent flame retardant system based on polyallylamine and polyphosphate and filled with TiO_2 nanoparticles. The latter are added with aim to reinforce the carbonaceous char layer formed. Indeed, previous studies have shown that the presence of nanoparticles in the bulk of the material to be protected can also catalyse the formation of char during the burning process [15]. The growth, topography and morphology of the deposited coating assemblies have been characterized using ellipsometry, atomic force microscopy and scanning electron microscopy. The thermo-oxidative stability of polyamide and polyester fabrics has been evaluated by thermogravimetric analyses. Then, the fire performance of 5, 10 and 15 quadralayers (QL) assemblies have been assessed and discussed.

2. Experimental

2.1. Chemicals and substrates

Poly(allylamine) hydrochloride (PAH) (Sigma–Aldrich, Mw = 120 000–200 000 g mol^{-1}) and sodium polyphosphate (PSP) (Across Chemicals, reference 256-779-4, Mw = 2800 g mol^{-1}) were dissolved at 1 mg mL^{-1} in 0.15 M of sodium chloride (NaCl) (Carl Roth, Mw = 58.44 g mol^{-1}) and 10 mM of tris(hydroxymethyl) aminomethane (Tris) (Euromedex, Mw = 121.1 g mol^{-1}) buffer solution (pH adjusted to 7.5 ± 0.1 with hydrochloric acid (Acros Chemicals, 36.5–37%). The negatively charged TiO_2 nanoparticles were prepared using titanium (IV) bis (ammonium lactato) dihydroxyde (TiBisLac) (Aldrich, reference 388165, Mw = 121.1 g mol^{-1} 50%, w/w) precursor, at 5 mM in 0.15 M of sodium chloride and 10 mM of Tris buffer solution, and just before starting each LBL deposition experiments in order to avoid a spontaneous formation of TiO_2 polycondensation. The addition of polycation (PAH) to the TiBisLac solution produced a spontaneous turbidity of poorly crystalline TiO_2 nanoparticles [16]. All solutions were prepared from doubly distilled water (Millipore Simplicity system, ρ = 18.2 MΩ cm). Woven polyamide 6.6 (PAf) (containing traces of Titanium from the manufacturing process) and woven polyester (PEf) fabrics have a thickness of 0.5 mm, a density of 60 and 140 g m^{-2}, respectively. They were purchased from Empa testmaterials (St. Gallen, Switzerlzand) and were used for thermal degradation and fire retardancy characterizations. Single-side-polished (1 0 0) silicon wafers (Siltronics Archamps, France) were used for film characterization by ellipsometry and AFM. All Si-wafers were cleaned with Hellmanex solution (2%, w/v) for 30 min in ultrasonic bath, rinsed with distilled water, diluted HCl (0.1 M) and distilled water again and then dried with N$_2$ before layer-by-layer deposition.

2.2. Layer by layer elaboration

The substrates (polyamide and polyester fabrics or silicon wafers) were immersed successively into solutions containing positive (PAH), negative (PSP), again positive (PAH) and negative (TiO$_2$) species (Fig. 1). Between each immersion step, the substrates were rinsed in order to remove weakly adsorbed species. The adsorption and rinsing step times were set at 1 min. It is worth to mention
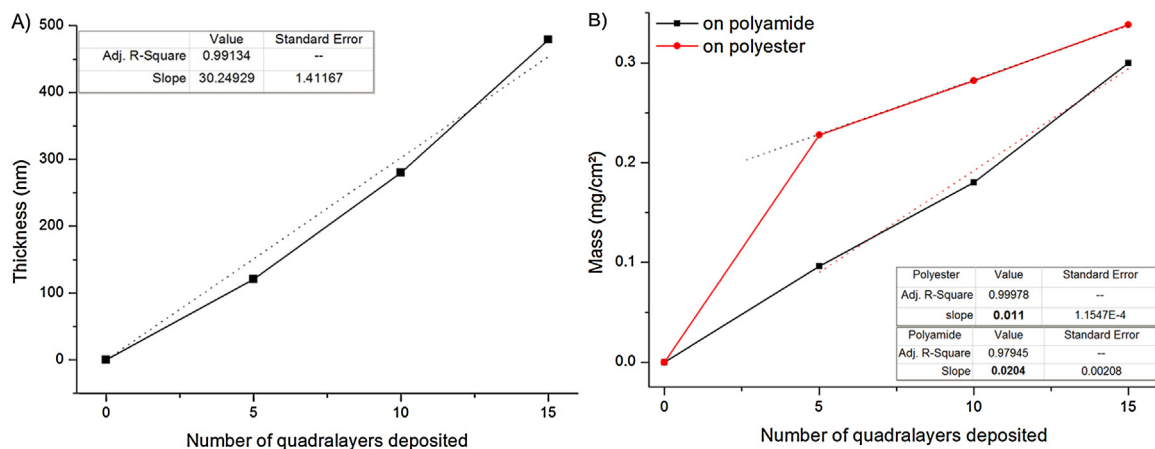
Fig. 2. Growth of (PAH-PSP-PAH-TiO$_2$)$_n$ assemblies (A) and mass (B) as a function of number quadralayers deposited.

that the samples were not blown dry between successive deposition steps. After the deposition of desired number of quadralayers (QL), the samples were rinsed in water and dried at ambient temperature.

2.3. Characterization

Dynamic light scattering measurements were performed using a NanoZS apparatus (Malvern Instruments, UK), equipped with a laser source operating at a wavelength of 632.8 nm, in order to measure the size and surface charge of TiO$_2$ nanoparticles. Light scattered by the sample was collected at an angle of 173°.

The thicknesses of the films, deposited on silicon wafers, were measured with an AUTO SE spectroscopic ellipsometer (Horiba, France) operating in the wavelength range 450–900 nm. In this spectral range neither the polyelectrolytes nor TiO$_2$ (E_g = 3.2 eV corresponding to an onset of absorption at λ = 387.5 nm) are absorbing light.

Atomic Force Microscopy (AFM) topographical images of the dried coatings, also deposited on silicon wafers, were acquired in the tapping mode with a Pico SPM microscope (Molecular Imaging) at a frequency of 1 Hz. Each image was acquired with a new pyramidal silicon tip. The images were acquired on films that were needle scratched just before image acquisition in order to have access to the topography of the deposits. The line profiles of the obtained sections were averaged over 30 line scans. The images were acquired over squares of 20 μm × 20 μm in area. The morphology of the (PAH-PSP-PAH-TiO$_2$)$_n$ films were measured by Scanning Electron Microscopy (SEM) with an environmental microscope (FEI-Quanta 200 type) coupled with an EDAX Genesis XM4i energy dispersive X-ray spectrometer (EDS) at an accelerating voltage of 10 kV, magnification ×50, ×1000, ×2000 and ×4000.

The contact angles of small water droplets (2 μL) on the pristine fabrics as well as on the fabrics coated with a (PAH-PSP-PAH-TiO$_2$)$_{15}$ film were obtained with a OCA20 goniometer (Dataphysics).

The thermal stability of the coatings and their effect on polyamide and polyester fabrics were investigated by thermogravimetric analysis (TGA) using a NETZSCH-STA 409 PC, operating in air environment under a 100 cm^3 min^{-1} gas flow. Approximately 7 mg of sample were loaded on alumina crucibles and the run was carried out in dynamic conditions at a constant heating rate of 10 °C min^{-1} between 30 and 1000 °C.

The fire retardancy was studied using a Pyrolysis Combustion Flow Calorimeter (PCFC) device (Fire Testing Technology, UK), according to ASTM D7309 method A. Each sample was approximately 7 mg and the test was performed under nitrogen atmosphere with a heating rate of 1 °C s^{-1} from 200 to 600 °C. All experiments were repeated in triplicate and the values are reproducible within ±3%.

3. Results and discussion

3.1. (PAH-PSP-PAH-TiO$_2$)$_n$ films characterization

Ellipsometry was used to follow the deposition of (PAH-PSP-PAH-TiO$_2$)$_n$ assemblies onto silicon wafers. On the other hand, since the fabrics are not characterized by a high reflection coefficient, ellipsometry cannot be used to follow the multilayer film deposition on their surface. Therefore, a more straightforward gravimetric method was used to investigate the growth (PAH-PSP-PAH-TiO$_2$)$_n$ assemblies on the surface and/or the pores of the fabrics. Fig. 2 shows the evolution of the thickness and mass gain as a function of the number of quadralayers (QL) deposited. On silicon, the coating thickness increases linearly with the number of quadralayers deposited with a thickness increment of 30 nm ± 1 nm QL^{-1}. In our previous work we have showed that the thickness increment for a (PAH-PSP) bilayer was of 10 ± 1 nm per bilayer on the same substrates and under identical experimental conditions [13] comment on this why such difference? The quadralayer assembly allows reaching a thickness of 479 ± 2 nm for assemblies made from 15 QL. The growth regime of the quadralayers was also followed by weighing both fabrics regularly, i.e. every 5 deposited quadralayers (Fig. 2B). On the polyamide fabrics, the film growth trend is similar to the linear trend observed with ellipsometry (Fig. 2A) for silicon substrates. However, on the polyester fabric, the weight gain increases quickly up to 5 QL (0.22 mg cm^{-2}) but then tends to a much slower linear regime with 0.011 mg cm^{-2} per QL deposited. This already emphasizes that the growth regime for a given combination of polyelectrolytes and nanoparticles is substrate dependent. In addition it shows that great care should be taken not to extrapolate the growth regime observed on silicon (Fig. 2A) to other substrates to be coated with an intumescent coating regarding their distinct wetting behavior as well as porosity which will be investigate hereafter.

The topography of the coatings, deposited on silicium wafers, was studied by AFM as shown in Fig. 3. A regular and continuous film made of the (PAH-PSP-PAH-TiO$_2$)$_n$ was observed at the surface. The root mean square roughness increases linearly with the number of quadralayers deposited with 124, 254 and 407 nm for 5, 10 and 15 QL, respectively. According to the roughness value obtained for our previous system (PAH-PSP)$_n$ without TiO$_2$ nanoparticles, (roughness = 27, 50 and 57 nm for 5, 10 and 15 BL respectively [13]),
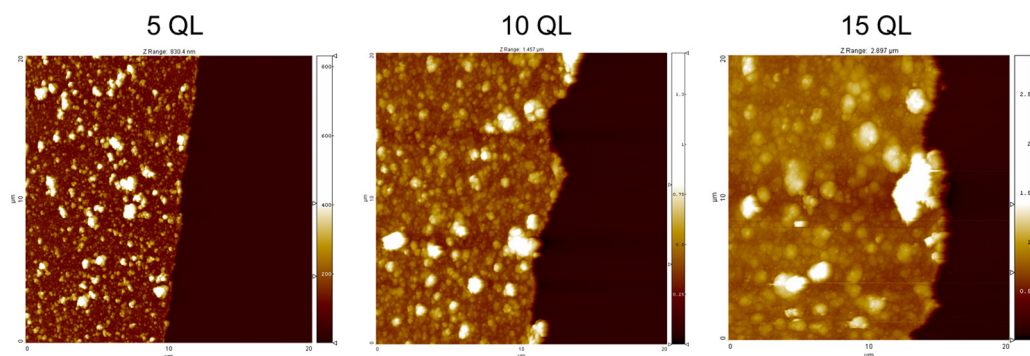
Fig. 3. AFM surface images of (PAH-PSP-PAH-TiO$_2$) coatings at 5, 10 and 15 quadralayers.

it is noticeable that the presence of TiO$_2$ nanoparticles could be the origin of the higher roughness value for the (PAH-PSP-PAH-TiO$_2$)$_n$.

To understand the difference of mass gain between the coatings deposited on polyamide and polyester fabrics, the cross sections of the coated fabrics were observed as depicted in Figs. 4 and 5. Fig. 4 shows the morphology of (PAH-PSP-PAH-TiO$_2$)$_n$ films at 5, 10 and 15 QL deposited on polyamide fabrics and the elemental analysis (carbon, oxygen, phosphorus and titanium) carried out, by EDS, on 15 QL samples. First of all, we can see that fibers of the woven polyamide fabrics form a compact network. The elemental analysis shows the presence of phosphorus (P) and titanium (Ti) elements on the external fibers: two components of the intumescent coating. In accordance with the EDS results, it is evidenced that all samples are well recovered by the coatings. In addition, the signal of phosphorus and titanium increases with the number of QL deposited (Fig. 4A). As in previous work [13] (Fig. 4C) we observe through the elemental analysis of the 15 QL assembly that the coating covers only the external fibers (Fig. 4B) and does not deposit on the internal fibers.

In Fig. 5, the coatings at 5, 10 and 15 QL deposited on polyester fabric were imaged. Contrary to the polyamide fabric, the polyester fibers present a scattered and pretty porous network which letting the (PAH-PSP-PAH-TiO$_2$)$_n$ assembly to be deposited not only

on the fibers exposed at the interface with the solution but also to diffuse into the bulk of the material. However, we observe that the coatings made 5 and 15 QL are deposited randomly in aggregates (more abundant for 15 QL) on some part of polyester fibers leading to a heterogeneous coating at the surface of the fibers. However, in the case of the coating at 10 QL only few defects were observed. The EDX spectrum displays an increase in the phosphorus and titanium signals as a function of the QL number. In the case of polyester fabric, the coatings were deposited randomly either in aggregates or in homogeneous film. The difference in morphology observed between the two kinds of fabrics is probably due to the difference in surface properties between polyamide and polyester fabrics (i.e.: wettability and surface energy [16]). Moreover, the polyester presents many disadvantages like hydrophobicity, electrostatic charge accumulation [17] which is not favorable for the deposition of hydrophilic species like PAH and PSP. Indeed water contact angles performed of the pristine fabrics were of $55 \pm 2°$ and of $0°$ on polyamide and polyester fabrics respectively (Fig. 6). The apparent perfect hydrophilicity of polyester leads indeed due to a fast permeation of all the water volume in between the fibers of the polyester. This is coherent with the finding that the polyelectrolyte coating penetrates in between the fibers (Fig. 5). The difference in the surface properties of both fabrics after deposition of polyelectrolyte films remains apparent not only on the SEM images and EDX
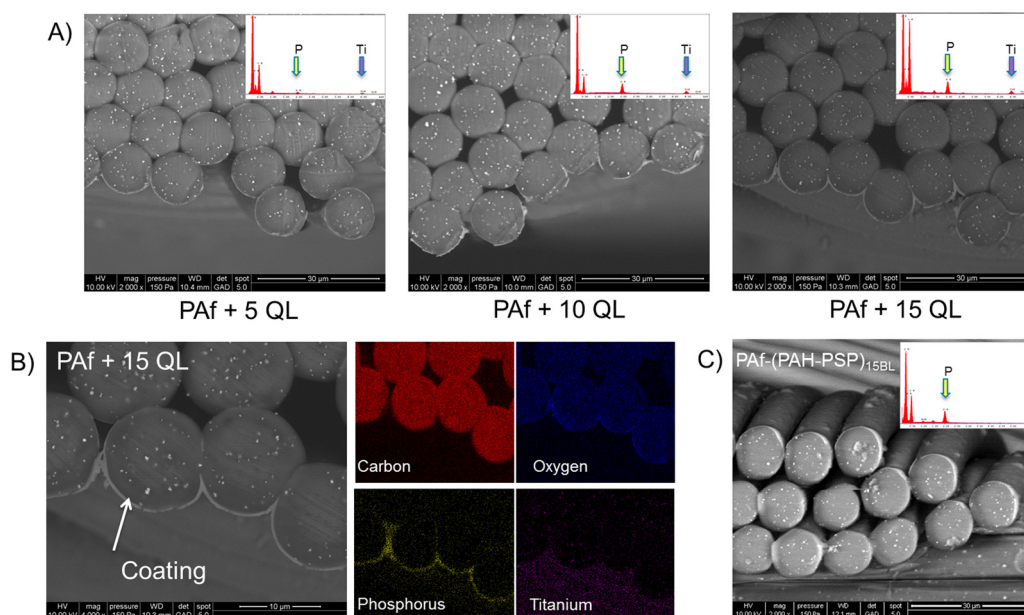

Fig. 4. SEM cross section of polyamide fabric coated with 5, 10 and 15 QL film and their EDX spectrum (A). SEM cross section of film at 15 QL and elemental analysis (C, O, P and Ti) (B). SEM cross section with EDX spectrum of PAf-(PAH-PSP) at 15 bilayers (C).
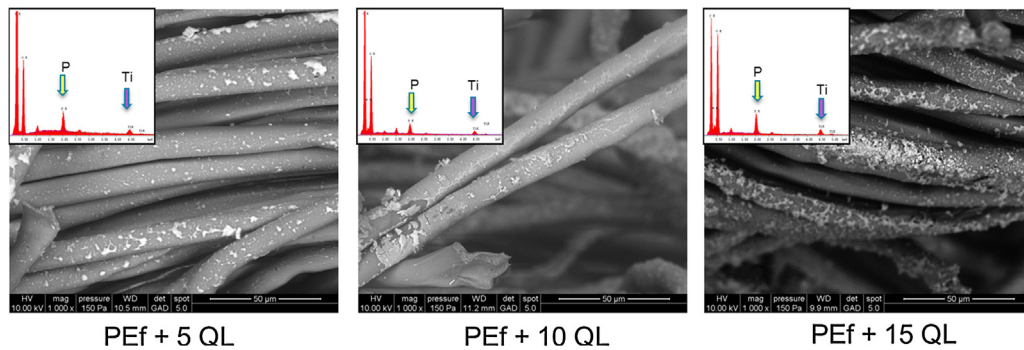
Fig. 5. SEM cross section of polyester fabric coated with 5, 10 and 15 QL film and their EDX spectrum.

spectra (Figs. 4 and 5) but also on the contact angle values of the "coated" fabrics: $(72 \pm 2°$ and $(52 \pm 4)°$ on polyamide and polyester after the deposition of a $(PAH-PSP-PAH-TiO_2)_{15}$ coating.

3.2. Thermal stability

The thermal stability of the $(PAH-PSP-PAH-TiO_2)_n$ assembly was evaluated by thermogravimetry under air at a temperature scan rate of $10°C min^{-1}$ (Fig. 7). The obtained data are summarized in Table 1. Fig. 7A shows TG and DTG curves of uncoated and coated polyamide fabrics (PAf). We determined the add-on of the samples corresponding to the percentage added by the coating to the virgin fabrics. In the case of PAf, the add-on values increase as a function of the number of QL deposited from 2, 3.8 and 6.2% for 5, 10 and 15 QL, respectively, while for polyester fabrics they were very close regardless the number of QL (2.4, 3 and 3.5% for 5, 10 and 15 QL, respectively). The uncoated PAf degrade in two steps: 440 and 550 °C as determined from DTG curves. It is well known that the thermo-oxidative degradation of polyamide leads to three principal reactions: (i) formation of N-acylamides, (ii) formation of N-formamides (due to C1–C2 bond scission) and (iii) oxidative dealkylation that yields carbonyl compounds [18]. At 5 QL, no meaningful modification was observed on the TG curves in comparison to the uncoated polyamide fabric, probably due to the low amount of coating deposited (add-on

at 5 QL = 2%). However, the polyamide fabric coated with 10 and 15 QL assemblies present three maximum degradation rates: 410, 450 and 550 °C (corresponds to maximum of DTG peaks curves). These coatings at 10 and 15 QL catalyze the thermal stability of PAf thanks to the presence of a large amount of phosphoric acid produced during the decomposition of the sodium polyphosphate [18]), as revealed by $T_{onset\ 10\%}$ values (Table 1a). Furthermore, the temperature of the degradation of all samples during the second step (main step of PAf degradation) is shifted to higher temperatures confirming therefore the stabilizing effect of coating ($T_{onset\ 85\%}$ values increase with the QL deposited). At 900 °C, no residue was observed for uncoated polyamide and PAf + 5 QL sample while the residual mass for 10 and 15 QL increases to ~2 and ~3% respectively. A comparison between the effect of the two coatings with and without TiO$_2$ shows that TiO$_2$ stabilizes the fabrics since the shift of the curve towards lower temperatures was much higher without TiO$_2$. Fig. 8 shows the TG (a) and DTG (b) curves of the uncoated and coated polyester fabric. The thermal degradation of polyester fabric occurs in two steps: 430 and 550 °C where the first step is attributed to β CH-transfer reaction and depolymerisation while the second one corresponds to oxidation of the residue formed during the first step [19]. All coated samples destabilize the degradation of polyester fabric as indicated by $T_{onset\ 10\%}$ values (Table 1b). For all samples, no residues were observed at 900 °C.

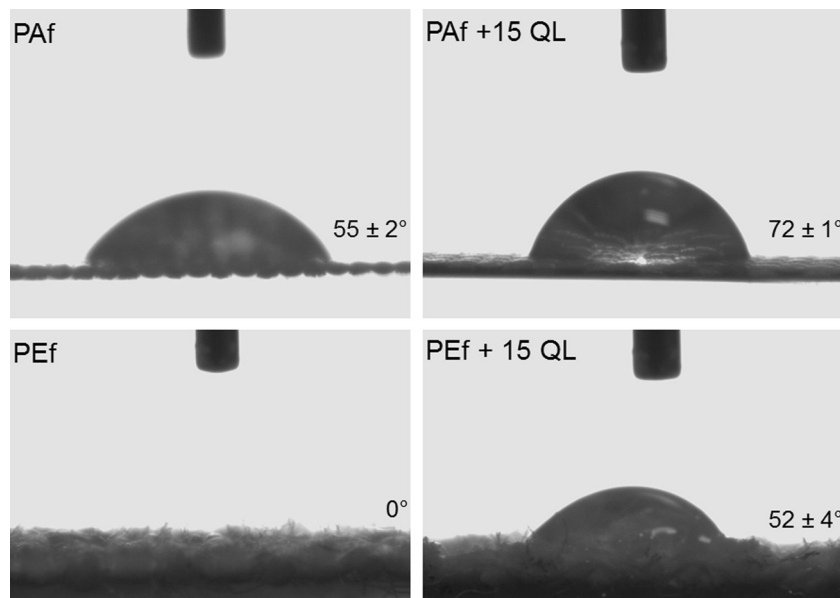**Fig. 6.** Water contact angle measurements on pristine and $(PAH-PSP-PAH-TiO_2)_{15}$ coated polyamide (upper row) as well as on pristine and $(PAH-PSP-PAH-TiO_2)_{15}$ coated polyester (lower row).
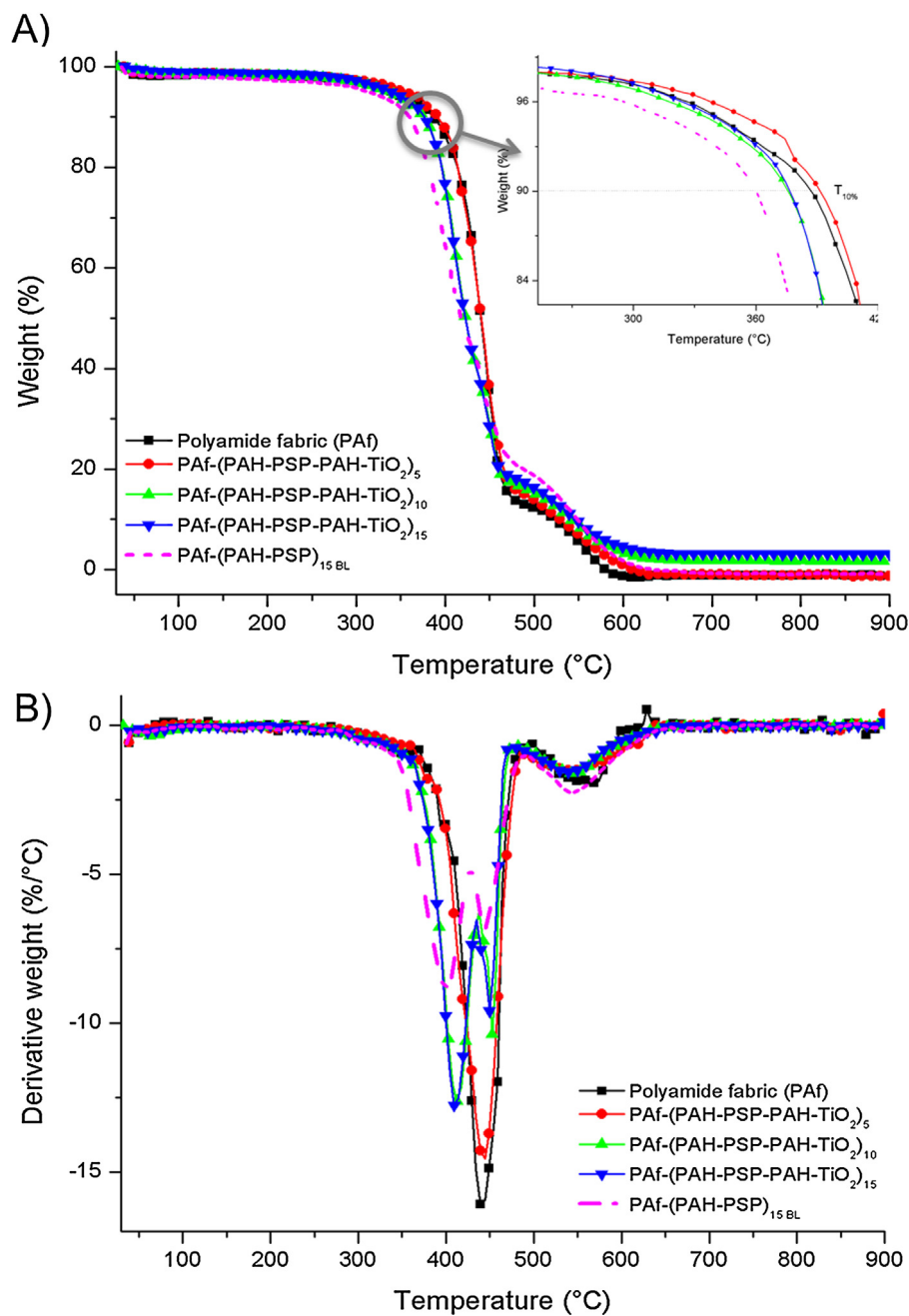
Fig. 7. TGA (A) and DTG (B) curves under air (heating rate: $10\,°C\,min^{-1}$) of uncoated and coated polyamide 6.6 fabric with 5, 10, 15 quadralayers and with (PAH-PSP) at 15 bilayers.

Table 1
TGA data for uncoated and coated polyamide (A) and polyester (B) fabrics with 5, 10 and 15 QL.

(A)	Add-on (%)	$T_{onset\ 10\%}$ (°C)	$T_{onset\ 85\%}$ (°C)	T_{max}^1 (°C)	T_{max}^2 (°C)	T_{max}^3 (°C)	Residue at 900 °C (%)
Polyamide fabric (PAf)	–	387	440	–	442	566	–
PAf + 5 QL	2	392	441	–	443	539	–
PAf + 10 QL	3.8	376	423	413	450	545	1.78
PAf + 15 QL	6.2	377	422	411	448	539	3.11

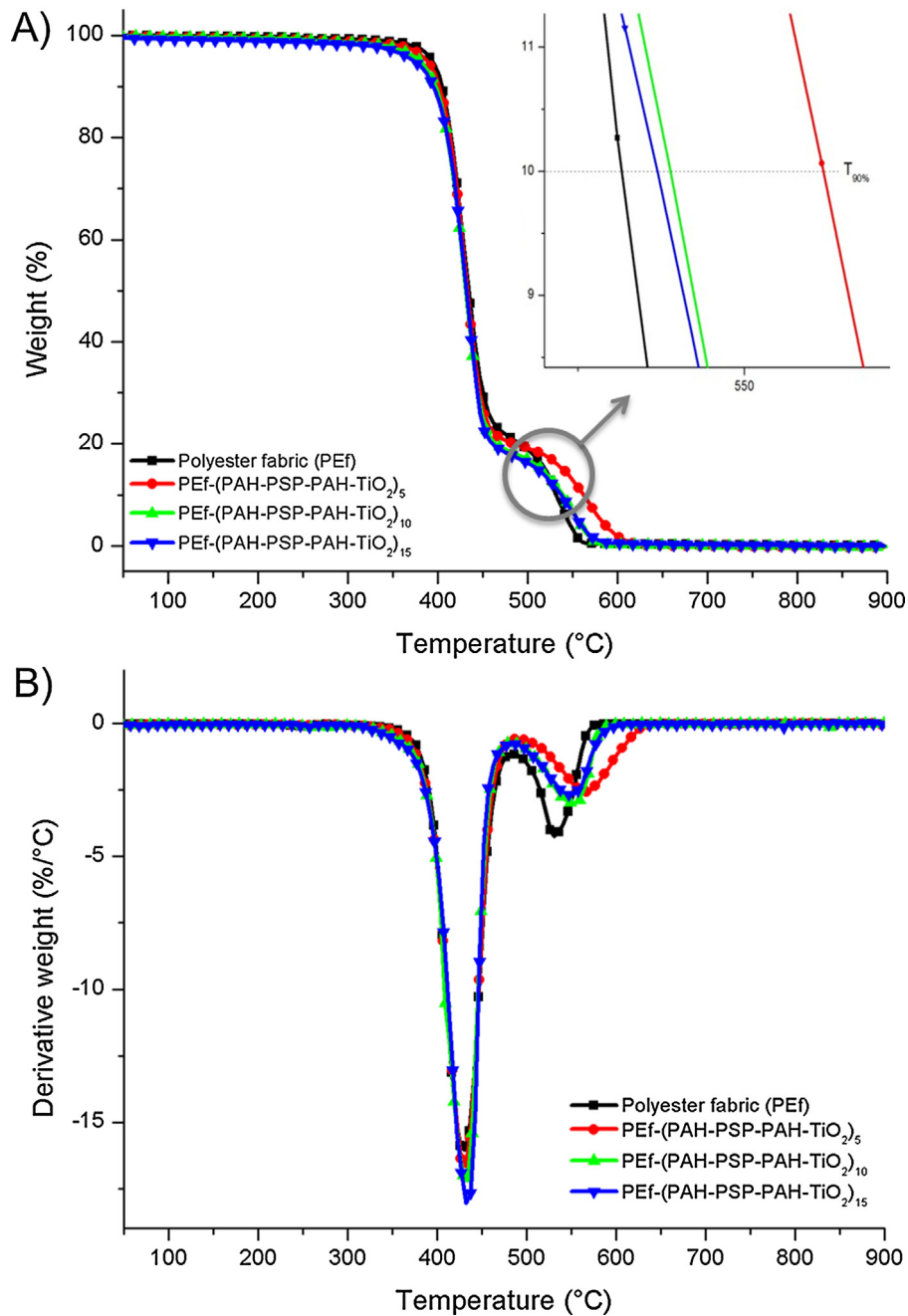| (B)	Add-on (%)	$T_{onset\ 10\%}$ (°C)	$T_{onset\ 90\%}$ (°C)	T_{max}^1 (°C)	T_{max}^2 (°C)	–	Residue at 900 °C (%)
Polyester fabric (PEf)	–	405	532	430	531	–	–
PAf + 5 QL	2.4	402	562	431	566	–	–
PAf + 10 QL	3	398	539	430	551	–	–
PAf + 15 QL	3.5	395	537	432	548	–	–

Fig. 8. TGA (A) and DTG (B) curves under air (heating rate: $10\,°C\,min^{-1}$) of uncoated and coated polyester fabric with 5, 10 and 15 quadralayers.

It is also apparent when comparing Figs. 7 and 8, that the coating has a much larger influence on the thermal behavior of polyamide than for polyester fabrics. This is could be related to the difference in morphological features of the $(PAH-PSP-PAH-TiO_2)_n$ coatings between the two fabrics (Figs. 4 and 5). In fact, the island like feature observed for the coating applied on polyester does not provide a homogenous protection of the whole surface of polyester.

3.3. Reaction to fire

First of all, in order to evaluate the potential of the (PAH-PSP-PAH-TiO_2)_n coatings deposited onto fabric substrates to act as flame retardants, samples of uncoated and coated polyamide and polyester fabrics at 15 QL were burnt using a lighter as showed in Figs. 9C and 10C, respectively. After burning, we

observe that the morphology of uncoated polyamide and polyester fibers changes from a fibrous state to a molten state along with the formation of a white residue in both cases (polyamide and polyester fibers) (see Figs. 9C and 10C). However in the case of both coated fabrics, we notice the formation of an expanded carbonaceous char after burning (see Fig. 8C and 9C). Yet, only PAf + 15 QL shows the formation of "bubbles" at the surface of substrate (see Fig. 8B, 30 000×), which is expected to act as a thermal barrier between the fire and substrate. Therefore, the fire performance of these intumescent (PAH-PSP-PAH-TiO_2)_n coatings at 5, 10 and 15 QL deposited on both fabrics were evaluated in depth using PCFC [20]. The recorded results are depicted in Fig. 11 and the corresponding data are gathered in Table 2. It is important to mention that the PCFC technique, measuring the heat release rate (HRR) of the pyrolysis products of the sample, provides
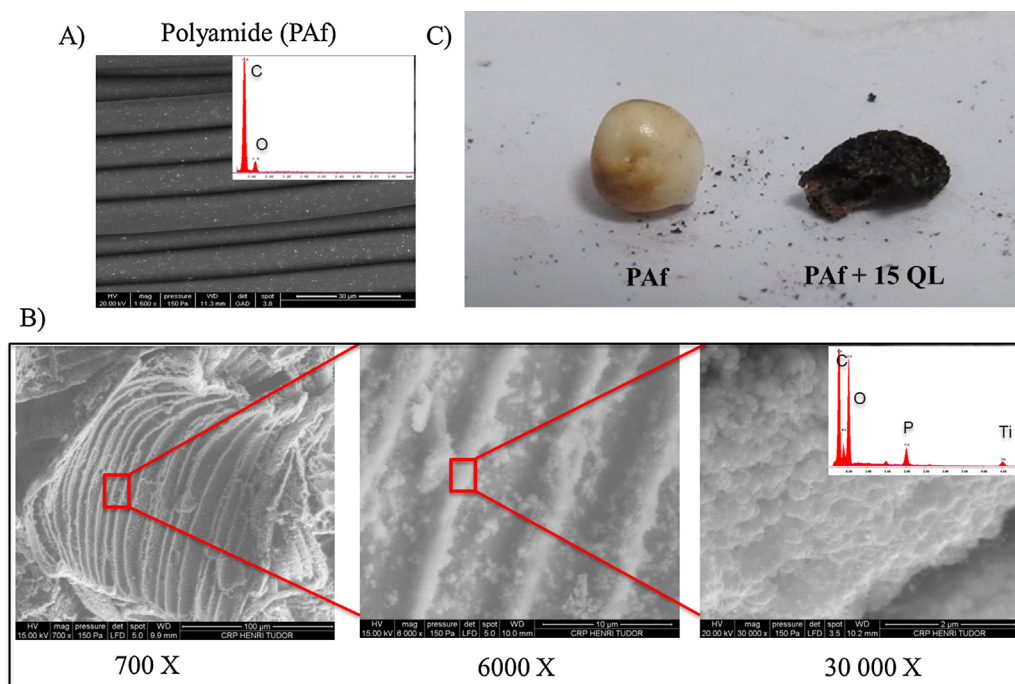
Fig. 9. SEM images of uncoated fabrics (A) and fabrics coated with15 QL assembly after burn testing at different magnification (B). Picture of coated and uncoated polyamide fabric after burning (C).

information about the mode of action of flame retardant acting in the gaseous phase.

The uncoated polyamide fabrics display a maximum pHRR of 492 ± 33 W/g and a decomposition temperature of 440 ± 4 °C. Only the coatings at 10 and 15 QL show a decrease of pHRR and a shift of decomposition temperature to lower values compared to the uncoated polyamide (Fig. 10A). The maximum reduction in pHRR (c.a. -26%) was observed for the PAf coated with 15 QL contrariwise

to PAf coated with (PAH-PSP) assembly at 15 bilayers displaying a reduction of pHHR of 30% as reported previously [13]. For the polyester fabric samples, no modification was observed in the decomposition temperature. However the pHRR decreases only down to 14% (at 15 QL), which is not really significant (Fig. 10B). Again this absence of significant effect may be due to the inhomogeneous deposition of the $(PAH-PSP-PAH-TiO_2)_n$ coating on the polyester fabric. We expected that the incorporation of TiO_2
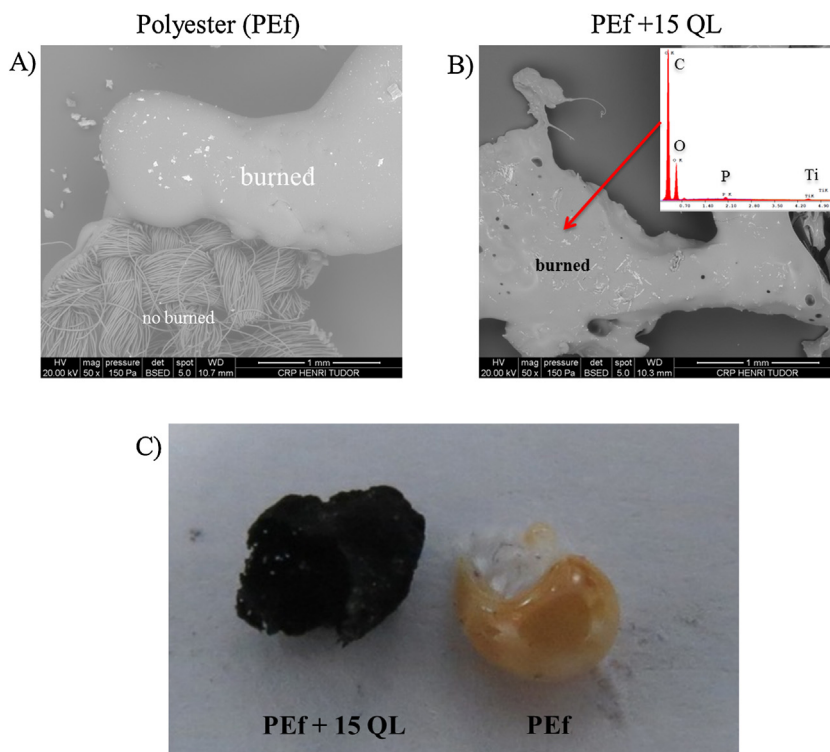

Fig. 10. SEM images of uncoated fabrics (A) and fabrics coated with15 QL assembly after burn testing (B). Pictures of coated and uncoated polyester fabric after burning (C).
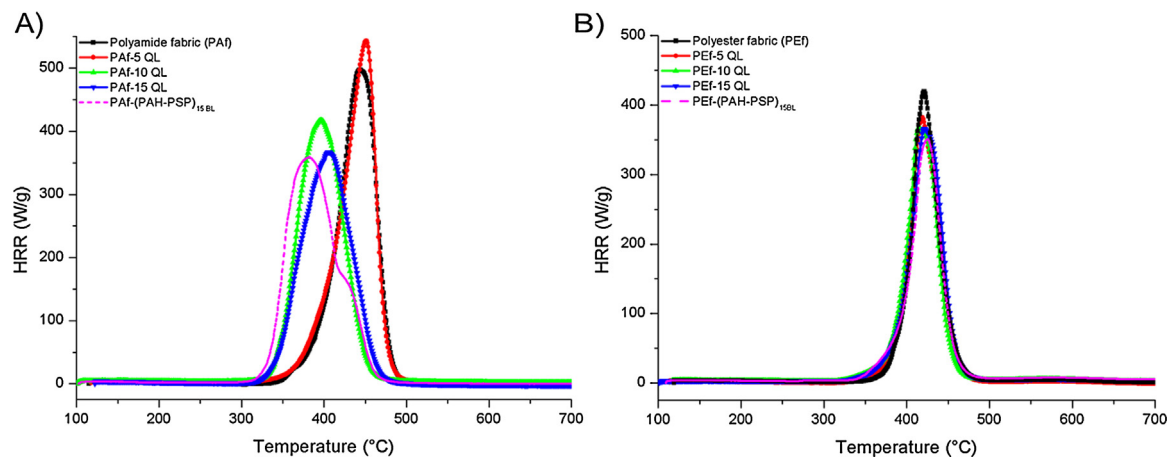
Fig. 11. Heat release rate curves as a function of temperature for coated and uncoated polyamide (A) and polyester fabrics (B).

Table 2
PCFC results of virgin and coated polyamide (A) and polyester (B) fabrics.

(A)	Peak HRR (W/g)	Peak HRR (°C)	% Reduction of pHRR (W/g)
Polyamide fabric (PAf)	492 ± 33	440 ± 4	–
PAf + 5 QL	544 ± 15	453 ± 4	–
PAf + 10 QL	435 ± 31	390 ± 6	12
PAf + 15 QL	363 ± 12	405 ± 4	26

(B)	Peak HRR (W/g)	Peak HRR (°C)	% Reduction of pHRR (W/g)
Polyester fabric (PAf)	421	421	–
PAf + 5 QL	380 ± 4	417 ± 3	10
PAf + 10 QL	372 ± 16	420 ± 4	12
PAf + 15 QL	361 ± 23	423 ± 1	14

generated through the polycondensation of Ti(BisLac) on direct contact with the PAH chains [16], would allow to produce a high reduction in the pHRR in comparison to a coating produced in the absence of nanoparticles. In our previous results, the (PAH-PSP) assembly at 15 bilayers decreased significantly the pHRR by 19% without use TiO$_2$ nanoparticles (see pink curve in Fig. 11) [13]. In the present case, with deposited 15 QL, which contains the equivalent of 15 PSP deposition steps, the pHRR is decreased by only 26% which is just slightly better than the result obtained in the absence of TiO$_2$ confirming that the presence of TiO$_2$ does not modify significantly the amount of deposited PSP.

4. Conclusion

The layer-by-layer technique has been used to design new intumescent flame retardant coatings in order to improve the reaction to fire of polyamide and polyester fabrics. This new assembly is constituted of polyallylamine, polyphosphate and TiO$_2$ nanoparticles. The thickness of the coatings deposited on silicon wafers exhibits a linear growth with a mass uptake of (PAH-PSP-PAH-TiO$_2$)$_n$ assembly, yet the growing of the same system on polyamide and polyester fabrics was different. This difference is mainly observed in the first 5 bilayers and may be due to the different surface properties mainly wettability and porosity between the fabrics. The morphology of coatings (before or after burning) has been studied by SEM to explain the different results obtained by PCFC. The coating covers homogenously all external fibers of polyamide whilst polyester fibers are covered partially with the formation of aggregates. Moreover, the presence of (PAH-PSP-PAH-TiO$_2$)$_n$ assembly has changed the degradation pathway of both fabrics. Finally, PCFC data showed that this new intumescent coating can improve the fire

behavior of polyamide fabric by reducing the pHRR of 26% for best samples (PAf + 15 QL). Nevertheless, The presence of TiO$_2$ in these particular (PAH-PSP-PAH-TiO$_2$)$_n$ coatings deposited on polyamide does not seem to significantly improve the fire retardant properties in comparison to the (PAH-PSP)$_n$ multilayer films. More importantly, it was found in this study that the efficiency of the designed coating in term of pHRR reduction depends strongly on the nature of the fabrics. This implies that more efforts are needed to extent the repertoire of polyelectrolyte multilayer films on different kinds of fabrics to find optimized coatings able to protect a given polymer against burning.

Acknowledgment

References

[1] Y.-C. Li, S. Mannen, A.B. Morgan, S. Chang, Y.-H. Yang, B. Condon, J.C. Grunlan, Intumescent all-polymer multilayer nanocoating capable of extinguishing flame on fabric, Adv. Mater. 23 (2011) 3926–3931.
[2] F. Carosio, J. Alongi, G. Malucelli, Flammability and combustion properties of ammonium polyphosphate-/poly(acrylic acid)-based layer by layer architectures deposited on cotton, polyester and their blends, Polym. Degrad. Stab. 98 (2013) 1626–1637.
[3] J. Alongi, F. Carosio, G. Malucelli, Influence of ammonium polyphosphate-/poly(acrylic acid)-based layer by layer architectures on the char formation in cotton, polyester and their blends, Polym. Degrad. Stab. 97 (2012) 1644–1653.
[4] G. Laufer, C. Kirkland, A.B. Morgan, J.C. Grunlan, Intumescent multilayer nanocoating, made with renewable polyelectrolytes, for flame-retardant cotton, Biomacromolecules 13 (2012) 2843–2848.
[5] G. Huang, J. Yang, J. Gao, X. Wang, Thin films of intumescent flame retardant-polyacrylamide and exfoliated graphene oxide fabricated via layer-by-layer assembly for improving flame retardant properties of cotton fabric, Ind. Eng. Chem. Res. 51 (2012) 12355–12366.
[6] F. Carosio, A. Di Blasio, J. Alongi, G. Malucelli, Green DNA-based flame retardant coatings assembled through layer by layer, Polymer 54 (2013) 5148–5153.
[7] S. Chang, R.P. Slopek, B. Condon, J.C. Grunlan, Surface coating for flame-retardant behavior of cotton fabric using a continuous layer-by-layer process, Ind. Eng. Chem. Res. 53 (2014) 3805–3812.
[8] F. Carosio, J. Alongi, G. Malucelli, Layer by Layer ammonium polyphosphate-based coatings for flame retardancy of polyester–cotton blends, Carbohydr. Polym. 88 (2012) 1460–1469.
[9] J. Alongi, F. Carosio, G. Malucelli, Layer by layer complex architectures based on ammonium polyphosphate, chitosan and silica on polyester-cotton blends: flammability and combustion behaviour, Cellulose 19 (2012) 1041–1050.
[10] A. Laachachi, V. Ball, K. Apaydin, V. Toniazzo, D. Ruch, Diffusion of Polyphosphates into (poly(allylamine)-montmorillonite) multilayer films: flame retardant-intumescent films with improved oxygen barrier, Langmuir 27 (2011) 13879–13887.
[11] A.A. Cain, C.R. Nolen, Y.-C. Li, R. Davis, J.C. Grunlan, Phosphorous-filled nanobrick wall multilayer thin film eliminates polyurethane melt dripping and reduces heat release associated with fire, Polym. Degrad. Stab. 98 (2013) 2645–2652.

[12] T. Zhang, H. Yan, M. Peng, L. Wang, H. Ding, Z. Fang, Construction of flame retardant nanocoating on ramie fabric via layer-by-layer assembly of carbon nanotube and ammonium polyphosphate, Nanoscale 5 (2013) 3013–3021.

[13] K. Apaydin, A. Laachachi, V. Ball, M. Jimenez, S. Bourbigot, V. Toniazzo, D. Ruch, Intumescent coating of (polyallylamine-polyphosphates) deposited on polyamide fabrics via layer-by-layer technique, Polym. Degrad. Stab. 106 (2014) 158–164.

[14] H.L. Vandersall, Intumescent coating systems, their development and chemistry, J. Fire Flammabil. 2 (1971) 140.

[15] J.W. Gu, G.C. Zhang, S.L. Dong, Q.Y. Zhang, J. Kong, Study on preparation and fire-retardant mechanism analysis of intumescent flame-retardant coatings, Surf. Coat. Technol. 201 (2007) 7835–7841.

[16] N. Laugel, J. Hemmerlé, N. Ladhari, Y. Arntz, E. Gonthier, Y. Haikel, J.-C. Voegel, P. Schaaf, V. Ball, Composite films of polycations and TiO_2 nanoparticles with photoinduced superhydrophilicity, J. Colloid Interface Sci. 324 (2008) 127–133.

[17] M. Bachurova, J. Wiener, Free energy balance of polyamide, polyester and polypropylene surfaces, J. Eng. Fibers Fabr. 7 (2012) 22–27.

[18] E. Guido, J. Alongi, C. Colleoni, A. Di Blasio, F. Carosio, M. Verelst, G. Malucelli, G. Rosace, Thermal stability and flame retardancy of polyester fabrics sol–gel treated in the presence of boehmite nanoparticles, Polym. Degrad. Stab. 98 (2013) 1609–1616.

[19] S.V. Levchik, E.D. Weil, M. Lewin, Thermal decomposition of aliphatic nylons, Polym. Int. 48 (1999) 532–557.

[20] R.E. Lyon, R.N. Walters, Pyrolysis combustion flow calorimetry, J. Anal. Appl. Pyrolysis 71 (2004) 27–46.